SURFACE GEOCHEMISTRY IN EXPLORATION FOR A BURIED GEOTHERMAL SYSTEM, SOCORRO, NEW MEXICO

Gregory T. Hill[1], Lara Owens[2], and David I Norman[2]

[1]Consulting Geologist
785 Andrew Lane
Reno, Nevada 89521 USA
e-mail: hillgreg@charter.net

[2]New Mexico Tech
Dept. of Earth and Environmental Science
801 Leroy Place, Socorro, New Mexico 87801

ABSTRACT

Selective extraction soil geochemistry is being used, along with geological, geophysical, and hydrological methods, to define a potential buried geothermal system in Socorro, New Mexico. Geophysical studies, along with projection of mapped geology suggest that a buried geothermal reservoir may occur approximately 2000-3000 feet below the surface. Soil geochemical patterns at the surface indicate the presence of a zone of thermal water at depth, as well as the presence of several important fault zones that may act as fluid conduits.

Two geochemical methods, enzyme leach (EL) and terrasol leach (TS), are being utilized to selectively dissolve specific Mn and Fe oxide and oxyhydroxide coatings on soil grains, without dissolving the bulk of the mineral substrate. The leach solutions are analyzed by ICPMS and up to 60 elements are reported with detection limits in the low parts-per-billion and parts-per-trillion levels. By effectively lowering background for most elements to levels that are well below those achievable by conventional extractions, subtle halo anomalies and linear highs in the ppb or ppt range can be resolved. At these and higher levels of concentration, many weakly bound elements contained on and within mineral coatings produce distinctive geochemical responses can be used to effectively target subsurface geothermal waters. In many cases, the anomalies are too subtle to recognize through conventional extractions such as aqua regia or four acid digestions.

The mechanisms of formation of surface anomalies detectable through selective extraction geochemistry are controversial and complex. At least two major processes are involved in forming the surface distributions: (1) upward migration of elements from the subsurface and (2) reconfiguration of elements already at the surface into forms that are soluble by the selective extraction being applied; in some circumstances, a small number of elements can be reconfigured into phases that are insoluble by some selective extractions. Each of these two components contributes varying amounts to the anomalous patterns depending on a large number of factors including depth of burial, climate, type of overburden, and fault and fracture density, to name a few. Electrochemical cells are key features that affect the element distributions. They are observable above buried geothermal systems, mineral deposits, and oil fields through measurements of pH, SP, conductivity, CO_2/O_2 fluxes, and trace and major element distributions. The advancement in understanding of these electrochemical cells enhances the ability to discover and explore geothermal systems.

An exploration well will test a high quality target developed by an integration of geological, hydrological, geophysical, and geochemical data.

INTRODUCTION

This study focuses on soil geochemistry above a blind geothermal prospect on the campus of the New Mexico Institute of Mining and Technology in Socorro, New Mexico. Baars et al. (this issue) discusses the project in detail. Campus lands to the immediate west of the city of Socorro lie in a designated Known Geothermal Resource Area (KGRA) in the uplifted fault block that forms Socorro Peak and its surroundings. Extensive past research has shown that heat flow is locally greatly elevated above background values for the region, reaching as high as 490 mW/m^2 on the eastern flank of the mountain, with computed thermal gradients as high as 350 ºC/km. Groundwater modeling studies suggest that the distribution of this elevated thermal

gradient is related to advective transport of heat by hydrothermal activity. Warm springs several miles to the south of the proposed drilling area also attest to the presence of a significant hydrothermal aquifer.

Trace elements in Geothermal Exploration

A wide variety of major and trace elements occur within geothermal fluids. Arsenic and Hg tend to have high concentrations in magma-heated fluids and at low concentrations, many other trace metals are also present in the fluids. The low detection limits of modern analytical technologies allow us to measure the concentrations of most elements on the periodic table in geothermal fluids. Through a compilation of Great Basin geothermal systems, Coolbaugh (2005) reports that magma-heated geothermal systems in the Great Basin contain higher amounts of As, Li, B, and Cs than amagmatic systems, and that both types of geothermal fluids are actively depositing Au.

Soil sampling techniques have been utilized for several decades in the search for geothermal resources. Mercury soil sampling techniques have been applied successfully to geothermal exploration for at least thirty years (White 1967; White et al., 1970; Matlick and Buseck, 1975; Christensen et al., 1980; Matlick and Shiraki, 1981; Matlick and Morris, 2005; Henkle et al., 2005). In a GRED II project at Lightning Dock in southwestern New Mexico, selective extraction geochemistry proved successful (Bowers, 2004 pers. comm.). Selective extraction soil survey techniques are used extensively in mineral exploration. In more than one case, Au exploration programs in covered terrains in Nevada have accidentally discovered buried geothermal systems through drilling based in part on surface geochemistry.

Selective Extraction Analyses and Patterns

Two selective extractions were utilized in the current study: enzyme leach (EL) and terrasol (TS). Both techniques are designed to selectively dissolve Mn and/or Fe oxides and oxyhydroxides while minimizing the leaching of the mineral substrate. The TS chemistry is designed to attack amorphous Mn and Fe phases and also dissolves a portion of the crystalline varieties of these minerals (Clark, pers. comm.). As a result, TS is considerably more selective than a conventional extraction and typically yields results that are about two orders of magnitude lower than total or near total digestions. EL is more sensitive than TS and typically yields results that are two to three times lower in magnitude than total or near total digestions. The EL chemistry utilizes the protein glucose oxidase to catalyze dextrose to gluconic acid and hydrogen peroxide (Clark, 1995) as shown in reaction 1.
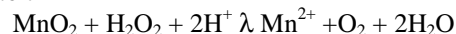
reaction 1
$$C_6H_{12}O_6 + O_2 + H_2O \, \delta \, C_6H_{12}O_7 + H_2O_2$$
dextrose + oxygen + water δ (glucose oxidase) δ gluconic acid + hydrogen peroxide

In turn, the hydrogen peroxide reacts with amorphous MnO_2 as shown in reaction 2, releasing trapped trace elements into the leach solution.

reaction 2
$$MnO_2 + H_2O_2 + 2H^+ \, \lambda \, Mn^{2+} + O_2 + 2H_2O$$

Because amorphous MnO_2 is much more reactive than the crystalline variety, once the amorphous MnO_2 is reacted, reaction 2 slows, the H_2O_2 content builds up to a low ppm threshold and reaction 1 also slows. Thus, the mineral substrate is only minimally reacted. In practice, the leach process is timed to allow for adequate leaching of the amorphous MnO_2 and minimize leaching of crystalline MnO_2.

Thus, background is effectively decreased allowing for low detection limits into the ppt or low ppb range for most elements. In addition to minimal leaching of the mineral substrate, the compositions of leach solutions are also affected by the dissolution of weakly bound cations, dissociation of salts, and hydrolysis. Relative to the total amount of material being dissolved, these processes contribute very little to conventional extractions, but their contributions to selective extractions can be significant. Additionally, repeated empirical observations indicate that significant reactions are taking place that increase or decrease the availability of certain elements to the leach solution. Many of the reactions taking place in these environments are not understood and are the subject of important ongoing research.

The decrease in background achieved by selective extraction techniques allows for the measurement of subtle anomalies that are well below threshold values of conventional extractions such as aqua regia. Many subtle changes in soil composition above blind geothermal systems, mineral deposits, and oil and gas reservoirs can be detected by selective extraction methodologies. In many cases, major soil changes, such as migration of Ca from a central low into a halo, also occur and these can be detected by conventional analyses. There are many factors that control the strength of a geochemical response above a subsurface body but in general terms, soil geochemical responses are more subtle for deeper bodies and therefore very weak extractions are necessary to detect anomalies associated with deep bodies. Anomalous soil geochemical patterns associated with shallowly buried mineral bodies are often readily detected by stronger leaches. Thus, dependent on geological conditions, there are opportunities to use combinations of extractions, ranging from strong to weak, to deduce three-dimensional geochemical depictions of the

subsurface. Pairing selective extractions, for this and other purposes, is being done successfully in mineral exploration (Hill et al., 2001).

EL and TS analyses of *B*-horizon soils reveal element patterns related to buried subsurface bodies that have geochemical contrast to the country rocks (Clark et al., 1990; Clark, 1993). Subtle oxidation and/or bio-oxidation of a buried reduced body produces a reduced chimney vertically above that body (Tompkins, 1990; Clark, 1993; Hamilton et al. 2004). Hamilton et al. (2004) have shown that variations in redox, pH, and SP are measurable in saturated glacial overburden above buried mineral deposits. Soil pH results are discussed in Baars et al. (this issue). The presence of this reduced chimney constitutes the establishment of an electrochemical cell and allows for the transport of volatile species from the subsurface. It also produces mineralogical changes involving elements that already exist at the surface. Some of the mineralogical changes remove elements from phases that are soluble by a particular solution and either remove them from the soil entirely, or place them into minerals that are insoluble in that solution (Hill and Clark, 2000). Thus, interpretation of selective extraction data requires consideration of transport of elements from the subsurface, and reconfiguration of those already at the surface.

Clark and Russ (1991) define a group of elements that they call the oxidation suite. This group comprises: Cl, Br, I, Mo, As, Sb, W, Re, V, Se, Te, U, and Th, and has since been expanded to include Au (Bob Clark pers. communication). Some or all of the oxidation suite elements tend to form distinctive halo patterns above subsurface bodies with significant geochemical contrast. In robust systems, these halos are typically zoned with respect to each other and can be nested, with concentric halos of different diameters being formed by the same element (Hill and Clark, 2000; Hill et al., 2001). Depletions in high field strength elements sometimes occur within the central low and commonly at the interface between a central low and a halo (Hill and Clark, 2000). Where robust electrochemical cells are present, some or all of the metals, rare earth elements, lithophile elements, and precious metals will also migrate into halo anomalies. The term oxidation anomaly is used to describe a coalescence of these geochemical patterns occurring above a slowly reacting body in the subsurface.

Oxidation anomalies are typically asymmetrical, and may require comparison of a number of trace element patterns before they become apparent. Recognizing nested halo patterns, zoning, and depletion can be of great assistance in vectoring toward the center of an anomaly. These features are also important in assessing the intensity of the system responsible for the formation of an oxidation anomaly.

Regional Geology

The Socorro Peak KGRA has a complicated geologic history involving the formation of two major lineaments: the Morenci lineament and the Rio Grande rift. The Morenci lineament is a pre-rift magmatic feature responsible for the many calderas and the associated ring fractures within the region, including the Socorro Caldera, which superimposes the Socorro Peak fault block to the south. Socorro Peak is an uplifted fault block associated with Rio Grande rift formation, bounded by a major N-S trending normal fault on the east side. The geology of the fault block includes Precambrian fractured granitic basement, Paleozoic limestones and shales, Oligocene volcanic lava flows and tuffs, and Tertiary alluvial-fluvial sediments (Popotosa formation). All units are capped at the mountain peak by rhyolite lava domes and tuffs from the most recent magmatic event associated with the Socorro Caldera (Chapin et al., 1978; Chamberlain, 1999). At the top and to the north of Socorro Peak, the volcanic and sedimentary units are mostly eroded, exposing the Precambrian and Paleozoic basement in the Wood's Tunnel region.

The local structural setting is complex. In addition to the Rio Grande Rift extensional faulting, the margin of the Socorro caldron passes a few hundred meters south of Socorro Peak. The Socorro Peak complex is cut by NE fractures of the transverse shear zone (Figure 1). South of Socorro Peak is in a major accommodation zone across which eastward-dipping normal faulting that occurs north of Socorro changes to westward-dipping normal faults south of Socorro (Chapin, 1989).

Mineral deposits, containing Pb, Ag, Ba, F, Au, W, V, As, and Br, have formed veins in the faults of the Socorro Peak rhyolite and Popotosa formation; some of which were heavily mined in the 1880s (Ennis, 1996). The rhyolitic tuffs within Socorro Peak also exhibit whole-rock enrichment of elements such as Ba, As, Sb, Cs, Pb and REE. This is thought to be the result of input from a hydrothermal source.

Hydrologic System

All available hydrologic and heat transport models for the Socorro region suggest that the flow of water and heat is transported from the west in deep-penetrating aquifers, which recharge in the La Jencia basin sediments west of Socorro Peak (Barroll and Reiter, 1990; Mailloux et al., 1999). The recharge penetrates to several kilometers depth, picking up heat from crustal sources (possibly magma bodies recently injected into the crust), then flows eastward up the tilted units which come to the surface in the Socorro Peak area, adjacent to the Socorro Canyon normal fault. As a result, the geothermal gradient is
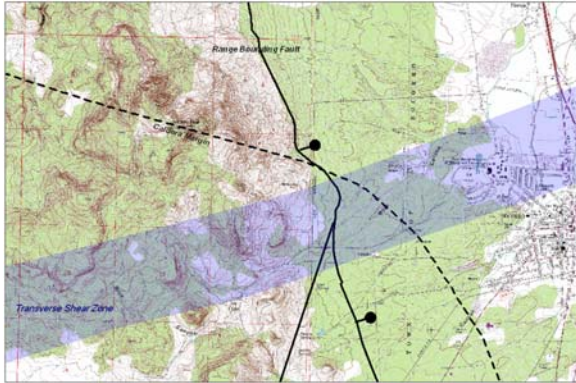
Figure 1. Major structural features of the Socorro Peak Complex: dashed line is the approximate location of the Socorro caldron, the solid line is the range bounding fault, and transverse shear zone is in the shaded area (Chapin et al, 1979).

steepest in the sediments, volcanics, and fractured basement rocks adjacent to the master fault. To the east of the fault zone, the basal fanglomerates of the Rio Grande rift valley are hundreds of meters thick, thus serving as a substantial hydrologic reservoir for multiple aquifers and an insulating buffer for any deeper geothermal system.

Design of Soil Survey and Sample Collection

Initially three east-west traverses were sampled. Each line was sampled in a few days. Sample-site locations were recorded by GPS, and the sample site was flagged. Three lines were done initially to evaluate the method. Two of the three lines revealed anomalies that clearly showed the location of an inferred fault (Chamberlain, 1999); hence the lines were extended and increased in number to five. When lines were extended two or three stations of the existing traverse were resampled to insure that subsequent sampling produced comparable results. In addition, replicate samples were taken every 20th sample. A total of 152 samples were collected from 136 sites (Fig. 2). Several stations that yielded very high values were also resampled and in all cases showed similar values (±25%). Uncertainty in values because of different sampling days is inconsequential considering that many elements show a range in values of three orders of magnitude or greater. Three samples have been removed from the data set because of suspected anthropogenic contamination. The removal of these samples does not substantially change the geochemical patterns but make the patterns discussed herein more readily recognizable.

Results and Discussion

A summary map illustrating the position and morphology of the oxidation anomaly is shown in Figure 3. Fifty-seven elements were detected by EL

and 52 by TS. Simple statistics, background values, and maximum contrast are listed in Table 1. Elements with maximum contrast ranging from 5680 to 10 include, in descending order: Pb, Zn, Mo, Cs, U, Hg, Cd, Tl, Co, Ni, I, Mn, Cu, Be, W, Ag, Cl, Sr, Ge, Zr, Nb, Bi, As, Re, Au, In, and Ti. Some of these elements are more concentrated in either EL or TS, but many show similar contrast (although considerably different absolute values) by both methods. Because the contrast is so high for many elements along the range front fault system, halo patterns can be difficult to discern in plots of the raw data. Some elements show responses of similar magnitude in the eastern and western portion of the oxidation anomaly (Figure 4). For others, truncating the geochemical data can lead to easier recognition of halo patterns (Figure 5).
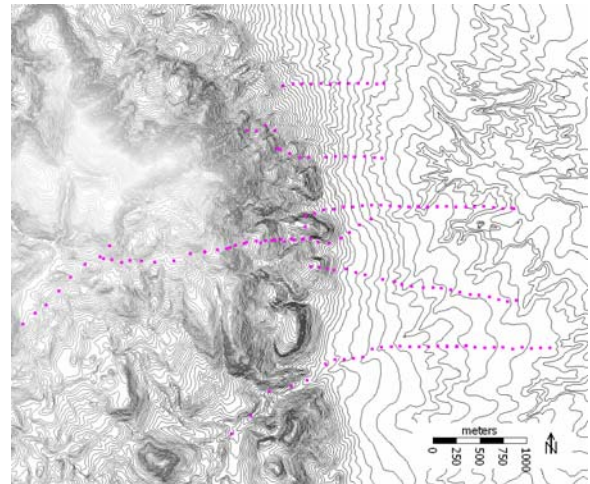

Figure 2. Soil survey locations on topographic map of survey area. Socorro Peak is at the center of the map.
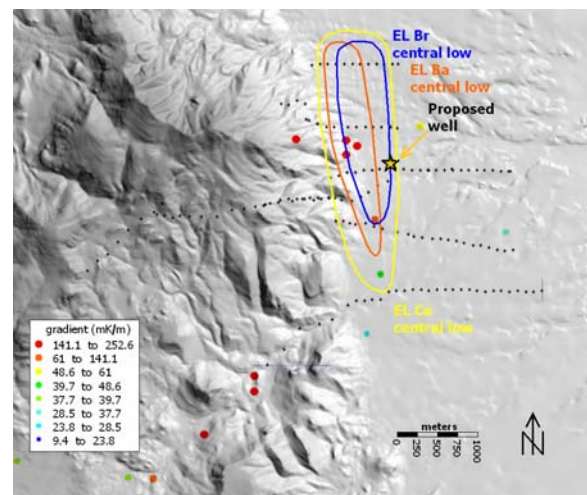

Figure 3. Summary map showing sample locations, outlines of central lows, geothermal gradient wells, and proposed well location overlaid on DEM.

Table 1. Simple statistics and background and contrast for determined elements.

Element	Cl	Cl	Br	Br	I	I	V	V	As	As	Se	Se	Mo	Mo
Method	EL	TS	EL	TS	EL	TS	EL	TS	EL	TS	EL	TS	EL	TS
Maximum	22700	n.d.	309	n.d.	481	n.d.	715	1820	716	3900	8	234	437	1990
Mean	3633	n.d.	63	n.d.	32	n.d.	158	398	85	569	3	102	25	70
Median	1000	n.d.	50	n.d.	18	n.d.	121	292	60	424	3	100	11	16
Std dev.	4468	n.d.	43	n.d.	52	n.d.	123	333	87	524	1	15	52	191
Background	1000	n.d.	40	n.d.	10	n.d.	100	250	60	300	3	100	10	5
Contrast	**23**	n.d.	8	n.d.	**48**	n.d.	7	7	**12**	**13**	3	2	**44**	**398**

Element	Sb	Sb	Te	Te	W	W	Re	Re	Au	Au	Hg	Hg	Th	Th	U	U
Method	EL	TS	EL	TS	EL	TS	EL	TS	EL	TS	EL	TS	EL	TS	EL	TS
Maximum	75.3	153	2	n.d.	416	1400	0.06	n.d.	0.29	25	n.d.	207	1.9	1290	7.0	852
Mean	18.9	38	1	n.d.	26	113	0.01	n.d.	0.03	3	n.d.	31	0.5	417.3	0.2	51.7
Median	15.4	33	1	n.d.	16	50	0.01	n.d.	0.03	3	n.d.	14	0.4	360	0.1	24.3
Std dev.	13.3	27	0.2	n.d.	39	159	0.01	n.d.	0.02	3	n.d.	40	0.3	236.4	0.7	93.1
Background	15	30	0.5	n.d.	15	50	0.005	n.d.	0.025	3	n.d.	2	0.25	300	0.1	20
Contrast	5	5	4	n.d.	**28**	**28**	**12**	n.d.	**12**	**10**	n.d.	**138**	8	4	**140**	**43**

Element	Zn	Zn	Pb	Pb	Ga	Ga	Ge	Ge	Ag	Ag	Cd	Cd	In	In
Method	EL	TS	EL	TS	EL	TS	EL	TS	EL	TS	EL	TS	EL	TS
Maximum	1510	70500	812	142000	2	125	4.2	24	n.d.	3460	61.6	5440	n.d.	11
Mean	25	2295	30	4095	1	35	0.3	7	n.d.	250	2.0	288	n.d.	1
Median	5	757	13	212	1	28	0.3	5	n.d.	125	0.9	128	n.d.	1
Std dev.	124	6047	78	13334	0	21	0.3	4	n.d.	365	5.2	514	n.d.	1
Background	5	100	1	25	0.5	30	0.25	5	n.d.	125	1	50	n.d.	1
Contrast	**302**	**705**	**812**	**5680**	4	4	**17**	5	n.d.	**28**	**62**	**109**	n.d.	**11**

Element	Sn	Sn	Tl	Tl	Bi	Bi	Co	Co	Ni	Ni	Cu	Cu
Method	EL	TS	EL	TS	EL	TS	EL	TS	EL	TS	EL	TS
Maximum	1.1	n.d.	1.2	237	1.1	37	237	29100	50	3840	324	25500
Mean	0.4	n.d.	0.1	5	0.4	4	16	1568	10	277	28	1339
Median	0.4	n.d.	0.1	3	0.4	3	8	595	7	50	21	735
Std dev.	0.1	n.d.	0.2	20	0.1	5	26	3162	10	563	33	2307
Background	0.4	n.d.	0.05	3	0.4	3	7	300	7	50	20	550
Contrast	3	n.d.	**23**	**95**	3	**15**	**34**	**97**	7	**77**	**16**	**46**

Element	La	La	Ce	Ce	Pr	Pr	Nd	Nd	Sm	Sm	Eu	Eu	Gd	Gd	Tb	Tb	Dy	Dy	Ho	Ho	Er	Er	Tm	Tm	Yb	Yb	Lu	Lu
Method	EL	TS	EL	TS	EL	TS	EL	TS	EL	TS	EL	TS	EL	TS	EL	TS	EL	TS	EL	TS	EL	TS	EL	TS	EL	TS	EL	TS
Maximum	8.8	3800	26.2	14000	2.8	1610	12.0	8420	2.8	2210	1.8	492.0	2.3	2150	0.4	n.d.	1.8	2010	0.3	388.0	1.0	1080	0.1	142	0.9	900	0.1	134
Mean	2.9	1545	6.0	3498	0.9	672	3.7	3233	0.8	799	0.5	185.5	0.7	725	0.1	n.d.	0.6	661	0.1	123.0	0.3	331	0.1	42.2	0.3	269	0.1	38
Median	2.4	1420	4.9	2490	0.7	623	3.1	3000	0.7	686	0.5	166.0	0.6	627	0.1	n.d.	0.5	564	0.1	105.0	0.3	279	0.1	34.5	0.2	217	0.1	30
Std dev.	1.6	941	3.8	2533	0.5	316	2.3	1510	0.5	388	0.3	81.8	0.4	362	0.1	n.d.	0.3	346	0.1	65.2	0.2	177	0.0	23.6	0.2	154	0.0	22
Background	2	1200	4	2000	0.7	600	2	2000	0.5	500	0.4	180	0.5	500	0.05	n.d.	0.4	500	0.05	100	0.2	300	0.05	35	0.2	200	0.05	30
Contrast	4	3	7	7	4	3	6	4	6	4	4	3	5	4	n.d.	5	4	7	4	5	3	4	5	5	3	4		

Element	Ti	Ti	Cr	Cr	Y	Y	Zr	Zr	Nb	Nb	Hf	Hf	Ta	Ta
Method	EL	TS	EL	TS	EL	TS	EL	TS	EL	TS	EL	TS	EL	TS
Maximum	146	5480	n.d.	1040	10.2	11900	9	5670	2	33	0.2	134	n.d.	2
Mean	53	1135	n.d.	208	3.6	3490	2	1143	1	7	0.1	26	n.d.	1
Median	50	561	n.d.	200	3.2	2940	1	700	1	4	0.1	17	n.d.	1
Std dev.	16	1209	n.d.	72	1.9	1925	2	1099	0	7	0.0	23	n.d.	0
Background	50	500	n.d.	200	3	2000	0.5	500	0.5	2	0.05	15	n.d.	0.5
Contrast	3	**11**	n.d.	5	3	6	**17**	**11**	4	**16**	5	9	n.d.	4

Element	Li	Li	Be	Be	Sc	Sc	Mn	Mn	Rb	Rb	Sr	Sr	Cs	Cs	Ba	Ba
Method	EL	TS	EL	TS	EL	TS	EL	TS	EL	TS	EL	TS	EL	TS	EL	TS
Maximum	129	732	4	686	n.d.	578	22100	2200000	153	2430	36100	232000	19.7	766	9530	365000
Mean	35	154	1	90	n.d.	252	3544	191185	31	861	2687	31325	0.3	55	2846	116274
Median	30	127	1	26	n.d.	250	2280	66700	26	789	2260	27100	0.1	42	2610	99900
Std dev.	22	105	0	148	n.d.	26	3984	334273	17	345	3082	23189	1.6	70	1587	64824
Background	30	120	1	20	n.d.	250	1000	50000	30	800	2000	25000	0.1	50	2000	100000
Contrast	4	6	4	**34**	n.d.	2	**22**	**44**	5	3	**18**	9	**197**	**15**	5	4

The base metals associated with mineralization at Wood's Tunnel, along the western margin of the oxidation anomaly, are extremely enriched in soils near the mine workings and also along the Socorro Canyon fault, along the range front. These metals also show strong responses in a zone well to the east The north-trending zones of metals enrichment occur within a robust oxidation anomaly involving a large number of elements. Some elements show clear indications of this anomaly while the responses of others are more difficult to discern. Some of the more distinctive responses involve EL Br, Ba, and Ce. These elements each show distinctive halo patterns that are of differing dimensions and are offset from each other by 100-200 m in an east-west sense (Figures 4-5). These relationships could be explained by the presence of a fault-bounded geothermal reservoir that is sourcing Ba from an upper portion and Br from a lower part of the aquifer.

Many other elements are also distributed into distinctive halo patterns, especially among the EL data. Strong structural control of the oxidation anomaly is evidenced by high-contrast peaks over known and suspected fault zones. Whereas both data sets exhibit strong responses above known and suspected fault zones, the TS data tend to show higher contrast than do the EL results above faults, and halos are difficult to recognize among most TS elements. Conversely, many elements liberated by the EL technique are distributed into halos and show somewhat lesser, but also strong, responses over structural zones. Some examples of structural control are as follows.

Figure 6 illustrates the TS Hg distribution. This element shows characteristics of both structural control and distribution into a halo. A northwest-trending fault zone is suggested by the TS Hg

response. TS Ti shows this pattern more distinctly (Figure 7), and when interpreted in conjunction with the digital elevation model (DEM), this structural zone appears to be through going in the region. Other extensive fault zones are interpreted by this methodology as well. For example, TS Au was detected along northwest-trending fault zones, one of which extends through the northwestern margin of the oxidation anomaly and the other parallels it to the west, near the crest of Socorro Peak (Figure 8). The TS V pattern suggests the presence of a third northwest-striking fault in the eastern part of the survey, as well as a northeast-striking fault that appears to structurally control the eastern margin of the oxidation anomaly (Figure 9). The structural interpretation based on soil geochemistry and the DEM conforms with many of the mapped faults. In a few areas however, the structural interpretation based on soils and the DEM varies somewhat with mapped structures in the area (Figure 10). It is suspected that some of the interpreted faults have little surface manifestation and are buried by young sediments or volcanic rocks.
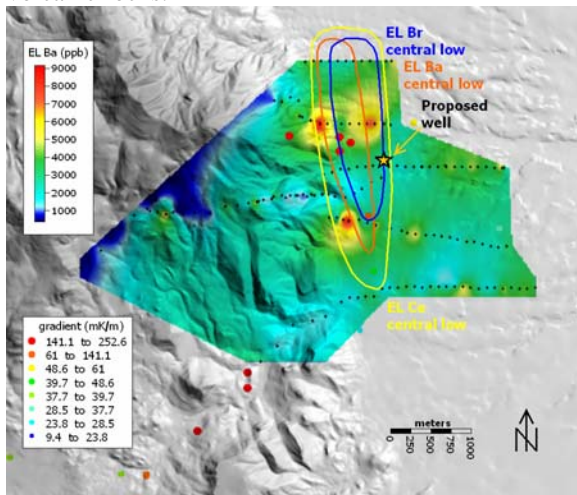
Figure 4. Distribution of EL Ba.
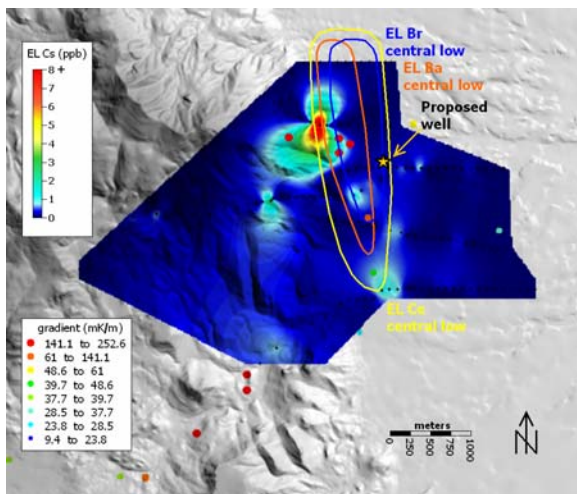
Figure 5. Distribution of EL Cs.
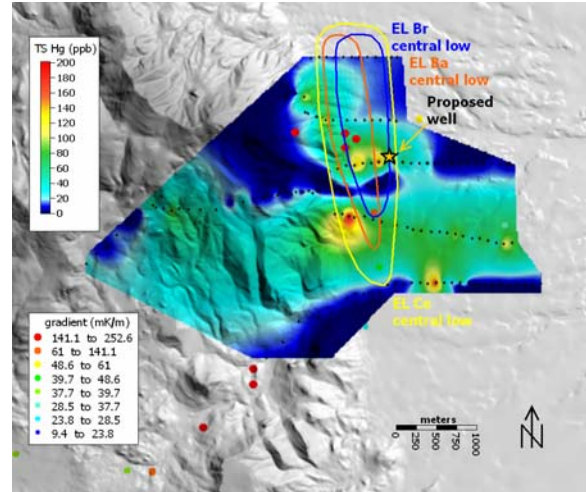
Figure 6. Distribution of TS Hg.

Breaks in the geochemistry occur near the center of the survey suggesting the presence of west-northwest and east-northeast-striking structural features related to the transverse shear zone and caldera margin. The distribution of samples does not allow for faults of these orientations to be seen in the geochemical data. Nonetheless, this component of the structural fabric is apparent in the geologic map (Figure 10).

Conclusions

Soil geochemical data define a well-formed, robust, structurally-controlled oxidation anomaly extending east from the range front. The center of the oxidation anomaly corresponds with high geothermal gradient values. Strong responses of Pb, Zn, and Cd suggest that subsurface geothermal fluids resemble those responsible for mineralization at Wood's Tunnel. Furthermore, high concentrations of Cl, Br, As, and Cs are found within the oxidation anomaly and are suggestive of a magma-heated geothermal fluid at depth. The proposed well location was chosen based on a combination of geological, geophysical, hydrological, and geochemical data, all of which independently indicate a similar target area.

References

Baars, R.M., Owens, L, Tobin, H., Norman, D.I., Cumming, W., and Hill, G.T., Exploration and targeting of the Socorro, NM direct use geothermal exploration well, a GRED III project, 2006, this issue.

Barroll, M.W. and M. Reiter, 1990. Analysis of the Socorro hydrogeothermal system: Central New Mexico, *J. Geophys. Res.*, **95(21)**, 949-963.
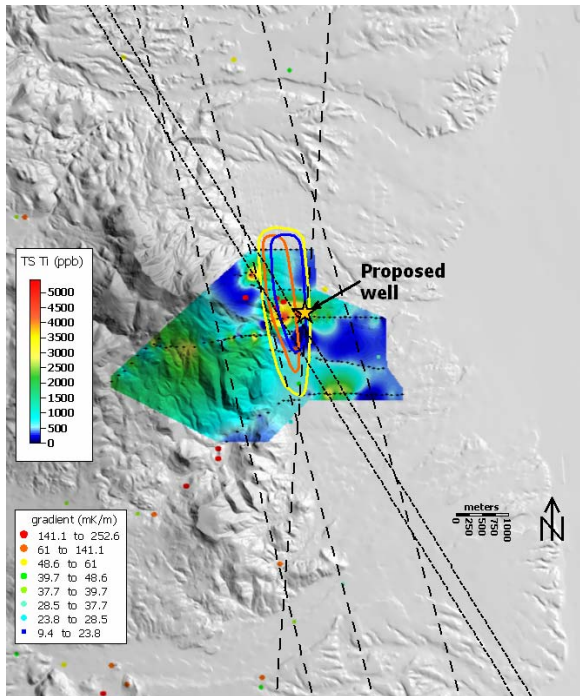
Figure 7. Distribution of TS Ti with summary of oxidation anomaly overlaid on DEM with interpreted structural zones based on surface geochemical data and topography.
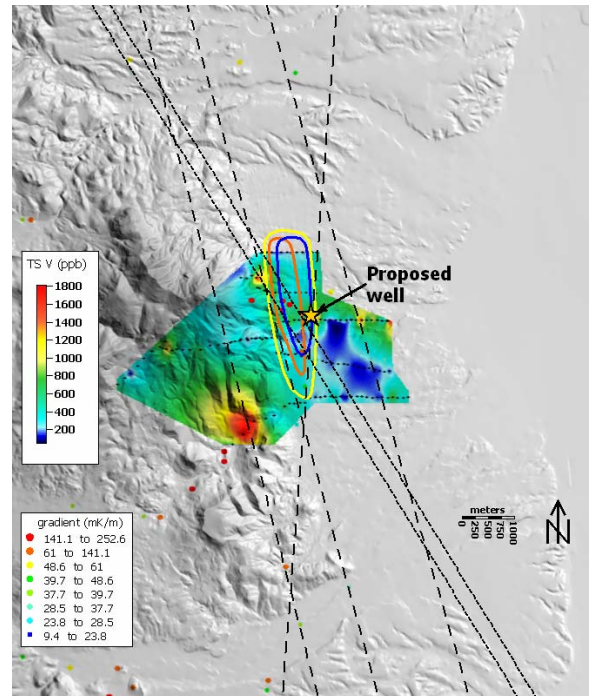

Figure 9. Distribution of TS V with summary of oxidation anomaly overlaid on DEM with interpreted structural zones based on surface geochemical data and topography.
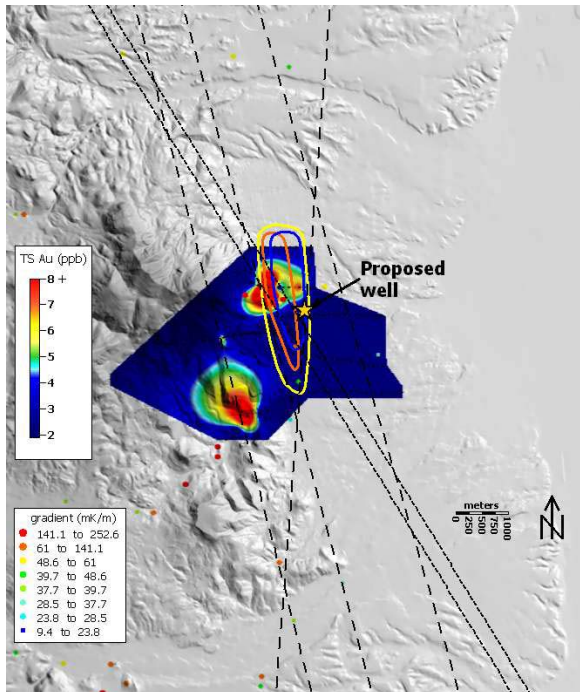

Figure 8. Distribution of TS Au with summary of oxidation anomaly overlaid on DEM with interpreted structural zones based on surface geochemical data and topography.
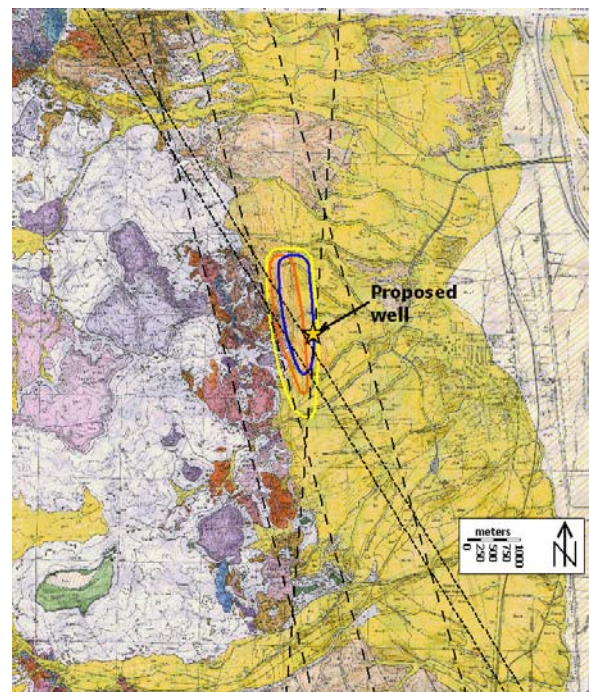

Figure 10. Summary of oxidation anomaly overlaid on geologic map of Chamberlain (1999) with interpreted structural zones based on surface geochemical data and topography.

Chamberlin, R.M. 1999, Preliminary geologic map of the Socorro quadrangle, Socorro County, New Mexico: *N.M. Bur. Geol. and Min. Res., Open-file Digital Map Series OF-DM-34*, 46p.

Chapin, C.E., A.R. Sanford, D.W. White, R.M. Chamberlin, G.R. Osburn, 1979. Geologic Investigation of the Socorro Geothermal Area, *N.M. Bur. Mines and Min. Res. Rpt. NMERDI* 2-65-2301.

Chapin, C.E., R.M. Chamberlin, G.R. Osburn, D.W. White, and A.R. Sanford, 1978. Exploration framework of the Socorro Geothermal Area, New Mexico, in *Field Guide to Selected Cauldrons and Mining Districts of the Datil-Mogollon Volcanic Field, Spec. Publi. N.M. Geol. Soc.*, **7**, 114-129.

Chapin, C.E. 1989. Volcanism Along the Socorro Accommodation Zone, Rio Grande Rift, New Mexico. p.46-57. In C.E. Chapin and J. Zidek (ed.) *Field Excursions to Volcanic Terrains in the Western United States,* **I** . N.M. Bur. Mines and Min. Res.

Christensen, O.D., Moore, J.N., and Capuano, R.M., 1980, Trace element geochemical zoning in the Roosevelt Hot Springs thermal area, Utah, *Geothermal Res. Council Transactions*, **4**, 149–152.

Clark, J.R., 1993, Enzyme-induced leaching of B-horizon soils for mineral exploration in areas of glacial overburden, *Trans. Instn. Min. Metall.*, (Sect. B: Appl. Earth Sci.) **102**, B19-B29.

Clark, J.R., Meier, A.L., and Riddle, G, 1990, enzyme leaching of surficial geochemical samples for detecting hydromorphic trace-element anomalies associated with precious-metal mineralized bedrock buried beneath glacial overburden in northern MN, in *Gold '90, Soc. Mining Eng., Chap. 19*, 189-207.

Clark, J.R. and Russ, G.P., 1991, A new enzyme partial leach enhances anomalies in pediment soils near buried gold deposits (abs.), *Assoc. Explor. Geochem. Symp.*, Reno, NV, USA.

Clark, J.R., 1995, Method of geochemical prospecting, United States Patent 5,385,827, 20 pp.

Coolbaugh, M.F., Arehart, G.B., Faulds, J.E., and Garside, L.J., 2005, Geothermal systems in the Great Basin, western United States: Modern analogues to the roles of magmatism, structure, and regional tectonics in the formation of gold deposits, *in* Rhoden, H.N., Steininger, R.C., and Vikre, P.G., eds., *Geol. Soc. of NV Symp. 2005,* 1063–1081.

Ennis, D.J., 1996. The effects of K-metasomatism on the mineralogy and geochemistry of silicic ignimbrites near Socorro, New Mexico. *Masters Thesis*. NMIMT.

Hamilton, S.M., Cameron, E.M., McClenaghan, M.B., and Hall, G.E.M., 2004, Redox, pH and SP variation over mineralization in thick glacial overburden. Part I: methodologies and field investigation at the Marsh Zone gold property, *Geochem.: Explor., Environ., Anal.*, **4**, no.1, 33-44.

Henkle, William R., Jr., Gundersen, Wayne C., and Gundersen, Thomas D., 2005, Mercury geochemical, groundwater geochemical, and radiometric geophysical signatures at three geothermal prospects in northern Nevada, *in* Rhoden, H.N., Steininger, R.C., and Vikre, P.G., eds., *Geol. Soc. of NV Symp. 2005,* 1147–1157.

Hill, G.T. and Clark, J.R., 2000, Enzyme leach signatures of the Marigold Eight North and Clay Pit gold deposits, Humboldt County, Nevada, *Geol. Soc. Nevada, Symp. 2000 Proceedings.*, 903-918.

Hill, G.T., Clark, J.R., and Lovstrom, K.A., 2001, Complementary selective extraction and biogeochemical patterns at the I-10 and Dragoon skarn/porphyry deposits, Cochise County, Arizona, Abs., *20th IGES Abstract Volume*, 79-81.

Mailloux, B., Person, M, Kelley, S., Dunbar, N., Cather, S., Strayer, L., and Hudleston, P., 1999. Tectonic controls on the hydrogeology of the Rio Grande Rift, NM, *Wat. Res. Resear.*, **35**, 2641-2659.

Matlick, J. S. and Buseck, P. R., 1975, Exploration for Geothermal Areas using Mercury, a New Geochemical Technique: in *Proc. 2nd U.N. Symposium on Development and Use of Geothermal resources*, Pazzotti, C., ed, **1**, 785–792.

Matlick, J. S. and Shiraki, M., 1981, Evaluation of the Mercury Soil Mapping Geothermal Exploration Techniques: *Geoth. Res. Council Trans.*, **5**, 95–98.

Matlick, S. and Morris, C., 2005, Updated geothermal exploration methods for Nevada, *in* Rhoden, H.N., Steininger, R.C., and Vikre, P.G., eds., *Geo. Soc. of NV Symp. 2005,* 1055–1061.

Tompkins, R., 1990, Direct location technologies: a unified theory, *Oil and Gas Jour.*, **Sept. 24,** 126-134.

White, D.E., 1967, Mercury and base-metal deposits with associated thermal and mineral waters, *in*: ed., Barnes, H.L., *Geoch. of Hyd. Ore Deposits.*, Holt, Rhinehart, and Winston, Inc., NY, NY, 575–631.

White, D.E., Hinkle, M.E., and Barnes, I., 1970, Mercury contents of natural thermal and mineral fluids, *US Geol. Surv. Prof. Paper 713*, 25–28.